Electroless Plating of Ultrathin Films and Mirrors of Platinum Nanoparticles onto Polymers, Metals, and Ceramics

Kurt P. Pernstich,*,† Michel Schenker,† Fabian Weibel,† Antonella Rossi,†,‡ and Walter R. Caseri†

Department of Materials, ETH Zurich, 8093 Zurich, Switzerland, and Dipartimento di Chimica Inorganica ed Analitica, Università degli Studi di Cagliari, 09100 Cagliari, Italy

ABSTRACT An organoplatinum precursor enables electroless deposition of platinum coatings, films, and mirrors on natural materials, synthetic polymers, metals, and ceramics by simply heating the precursor solution to temperatures of 80 °C or above. The films are comprised of densely packed platinum nanoparticles of 1−5 nm in size; they are flexible and electrically conducting and have pore sizes in the nanometer range.

KEYWORDS: platinum nanoparticles • ultrathin films • electroless plating • platinum mirror • nanoporous platinum • metallization of polymers

INTRODUCTION

In contrast to the electroless preparation of mirrors of noble metals such as gold or silver, which has been applied for centuries (1−3), employing this technique to produce platinum mirrors and films appears to be more difficult, and related reports are sparse (4−6). Conventional ways to deposit platinum films include gas-phase methods, electrochemical deposition, and the synthesis and subsequent deposition of nanoparticles, often in conjunction with a conducting matrix material. Yet, generating stable and highly dispersed films of platinum nanoparticles on solid or porous supports is still a major challenge and a subject of current interest, e.g., to improve the performance of fuel and solar cells (see, e.g., refs 7−12).

While electroless deposition methods are usually limited to a narrow range of substrate materials, the method described in the following enables coating of a universal range of substrates, i.e., polymers, metals, ceramics, and natural materials, notably without special surface pretreatment. Interestingly, the platinum films are porous with pore sizes in the nanometer range, which is in stark contrast to solid platinum films deposited with other methods and might enable novel membrane−electrode assemblies used in fuel-cell technology. In addition, the ultrathin films are electrically conducting and flexible, and they can be deposited as semitransparent films or as highly reflecting mirrors.

In the method presented, a dissolved organoplatinum precursor is converted at moderately low temperature (≥80 °C) to platinum nanoparticles that in situ adhere to immersed substrates without the need for additional ligands covering the nanoparticles. The particles assemble themselves into a densely packed, electrically conducting film with nanometer-sized pores, thereby eliminating the need for an additional electrically conducting matrix material, as is often required with other techniques.

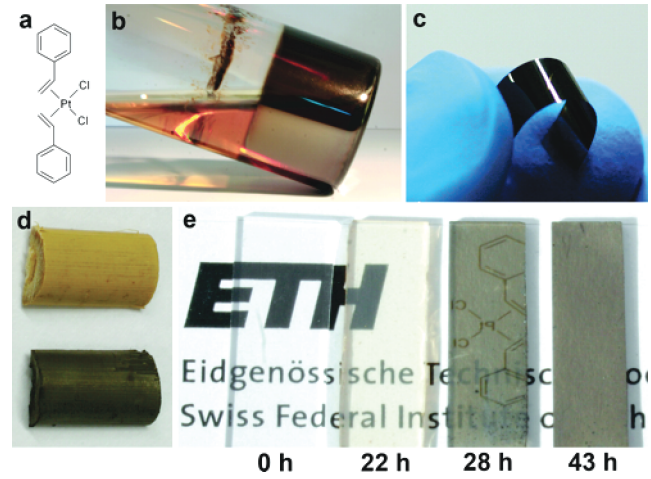

FIGURE 1. (a) Molecular structure of the precursor, which when dissolved in toluene and heated to 80 °C, forms platinum films on, e.g., the wall of a glass vessel (b). A broad range of substrates can be platinized, for instance, PET, resulting in a flexible mirror (c) or bamboo (d; before and after platinization). The film thickness varies with the deposition time as illustrated in part e, where the appearance of the deposited films varies from nearly transparent (22 h), to semitransparent (28 h), to highly reflecting (43 h).

The precursor, *cis*-dichlorobis(styrene)platinum(II) (Figure 1a), was dissolved in toluene at 80 °C and kept there for up to 7 days. Initially, after 22−24 h, a brownish, semitransparent *primary film* was deposited onto the walls of the glass vessel and onto immersed substrates. After heating for 2−3 days, a brownish, slightly bronze (Figure 1b) or shiny silvery (Figure 1e) film formed. This procedure requires little manual

* E-mail: pernstich@alumni.ethz.ch.
Received for review December 22, 2009 and accepted February 16, 2010
† ETH Zurich.
‡ Università degli Studi di Cagliari.
DOI: 10.1021/am900918y

and technical effort, and it is applicable to a wide range of substrates including *ceramics* [glass, photosensitive glass (Foturan), alumina, and Si/SiO_2 wafers], *metals* [nickel and gold], *synthetic polymers* [poly(ethylene terephthalate) (PET; Figure 1c), a polyimide (Kapton), Nylon 6.6, poly(*p*-phenylene sulfide), poly(tetrafluoroethylene) (solid and porous PTFE), cross-linked polystyrene, and a polymer electrolyte membrane (13) used in fuel cells], and *natural products* [cellulose, bamboo (Figure 1d), and carbon (graphite foil)].

While the appearance of the platinum films on these substrates varied from a shiny silvery nature (e.g., on glass, PET and Kapton) to bronze or black (e.g., on porous PTFE), all films adhered well to the substrates and were continuous and electrically conducting (if thick enough).

The thickness of the deposited film could be influenced, among others, by the *cis*-[$PtCl_2(sty)_2$] concentration, the solution temperature, and the deposition time, as illustrated for the latter case in Figure 1e. The films shown were grown using 7.5 mg of *cis*-[$PtCl_2(sty)_2$] per mL of toluene for respectively 22, 28, and 43 h at 80 °C. Once film deposition commenced, it was found to be rather rapid, with a visible thickness increase within 4−6 h, as evidenced by a changing appearance from nearly transparent (22 h) to semitransparent (28 h); see Figure 1e. The film formation was found to be a temperature-activated process, and the time required to form a primary film was reduced from 22 h at 80 °C to 5 h at 100 °C, while no primary film formed after 1 week at 60 °C. Similarly, the final platinum film formed after 16 h at 100 °C instead of 42 h at 80 °C.

On a microscopic scale, the films were found to be comprised of platinum nanoparticles, as is exemplarily shown in Figure 2 for a film grown onto Kapton and onto a carbon-coated transmission electron microscopy (TEM) grid. Interestingly, Figure 2a reveals the presence of two distinct layers. The close-up in Figure 2b shows that a first layer, referred to as the *primary film*, has a thickness of 10−15 nm and is comprised of particles with ≈1 nm diameter. The particle size increased to 3−5 nm in the successively grown layer, here of 60−65 nm thickness, designated as the *secondary film*. Crystalline platinum particles can be identified by Moiré patterns (stripes), as shown in the inset in Figure 2b. Primary particles (1−3 nm) also formed on a ruptured and coiled-up membrane of a carbon-coated TEM grid, as shown in Figure 2c, which also shows that some slightly larger particles (3−5 nm) agglomerated and formed three-dimensional clusters.

Scanning electron microscopy (SEM) images reveal a similar picture, where isolated clusters similar to those in Figure 2c were observed in a film deposited onto glass for 22 h, as shown in Figure 3a. These isolated structures are approximately spherical, as revealed by atomic force microscopy (not shown). The magnified view in Figure 3b reveals the granular structure of the clusters and also of the space between, which is supposedly covered with a platinum nanoparticle film because no imaging artifacts due to charging by the electron beam were observed [see also X-ray photoelectron spectroscopy (XPS) results below]. After a slightly longer deposition time (28 h), the clusters seen in Figure 3a seem to be overgrown by a continuous platinum nanoparticle film (Figure 3c), and overgrown clusters were also observed in TEM images. Also for longer deposition times, film formation appears to be a cyclic process of cluster growth and overgrowth. The film between clusters appears coarser for longer deposition times (Figure 3d) and also for

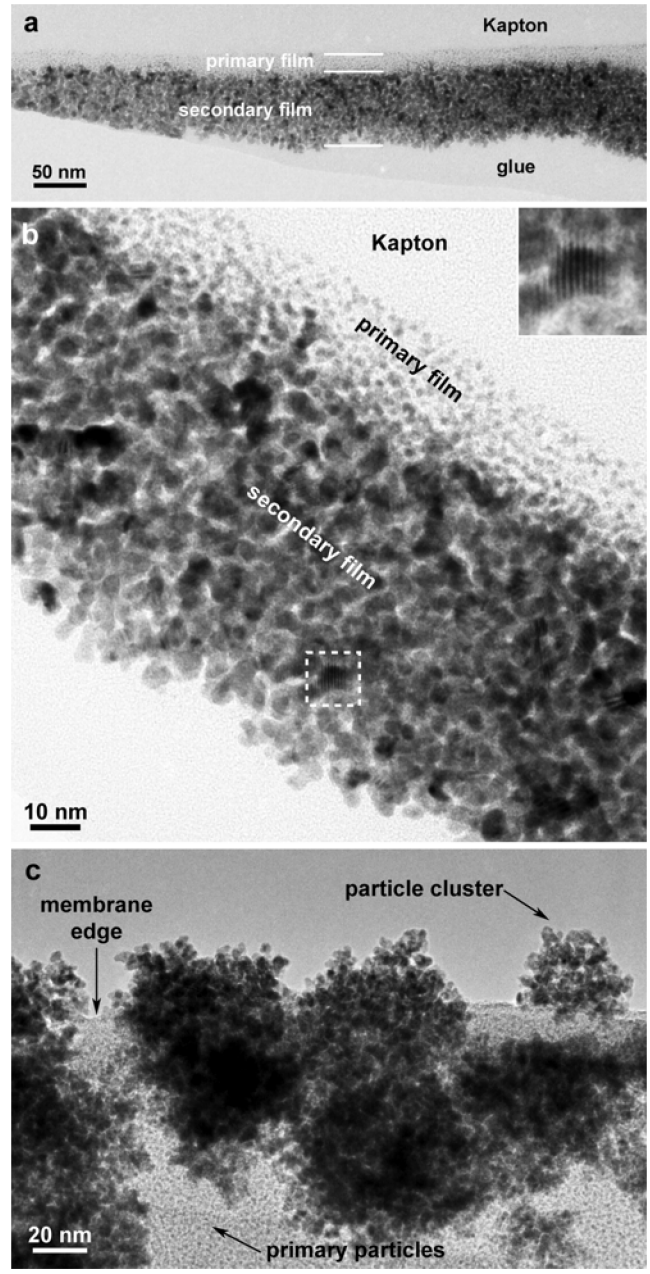

FIGURE 2. TEM images of a cross section of a platinum film deposited onto Kapton (a and b) and onto a carbon-coated TEM grid, where the membrane ruptured and coiled up (c). (a) Distinction between primary and secondary films comprised of nanoparticles of different sizes. The magnified view in part b demonstrates the porosity of the film and shows that particles in the primary film (10−15 nm thickness) are ≈1 nm in diameter and might have penetrated the Kapton, while particles in the secondary film (60−70 nm thickness) are 3−5 nm in diameter. Also, crystalline grains (dashed square) can be identified as shown in the inset of part b. (c) Primary platinum nanoparticles (1−3 nm) grew on the carbon membrane, and agglomerations of slightly larger particles (3−5 nm) formed three-dimensional clusters.

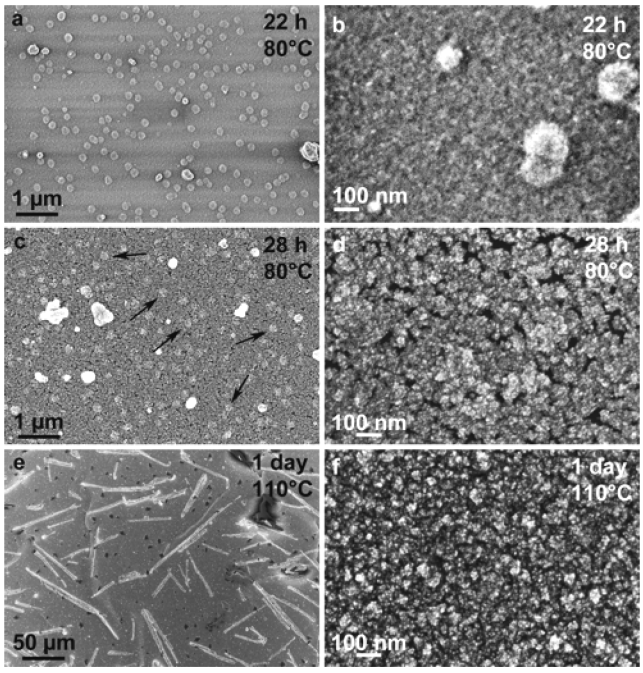

FIGURE 3. SEM images of films deposited at 80 and 110 °C onto glass for different times. After 22 h, isolated clusters formed on the surface (a). These clusters, as well as the platinum film between, are granular and comprised of nanoparticles (b). The arrows in part c mark a selection of brighter spots that are supposedly overgrown clusters. The film between clusters becomes coarser for increased deposition time (d) and also for a higher deposition temperature (f). A higher deposition temperature also leads to the formation of large needles and black precipitates on the surface (e).

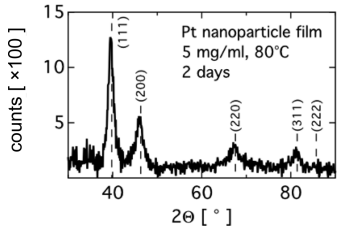

FIGURE 4. XRD pattern of a platinum nanoparticle film electroless deposited onto glass. The diffraction peaks correspond to elemental platinum.

an increased precursor concentration (not shown). Increasing the deposition temperature results in the formation of large needles and black precipitates, possibly platinum black, on the surface of the film (Figure 3e) and also to coarse film between these needles, as shown in Figure 3f. The growth velocity of the nanoparticles, respectively of the films, can therefore be tuned by varying the deposition temperature and precursor concentration. In annealed films (<400 °C), SEM revealed the formation of some cracks, possibly due to the different thermal expansion coefficients, but other than that, the film morphology on the length scale observed with SEM remained essentially unaltered.

X-ray diffraction (XRD) patterns recorded of a film deposited for 2 days onto glass under typical conditions (cf. the Experimental Section) are shown in Figure 4. The diffraction peaks correspond to (face-centered-cubic) elemental platinum, as illustrated with the dashed lines in Figure 4. From the peak width, a particle size of 10 nm was

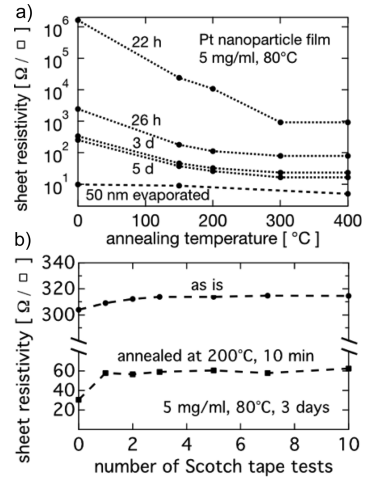

FIGURE 5. (a) Dependence of the sheet resistivity on the deposition time and annealing temperature. The sheet resistivity decreased by more than 3 orders of magnitude with increasing deposition times in as-deposited films. It also decreased upon annealing and is similarly low as in a 50-nm-thick thermally evaporated platinum film. (b) The sheet resistivity remains essentially constant for repeated Scotch tape tests, demonstrating the good adherence of the platinum films, here to glass.

estimated, which is similar to the particle size determined with TEM in a film deposited onto Kapton.

In order to substantiate the XRD results, survey XPS spectra were collected on a series of samples after various deposition times ranging from 2 h to 7 days. These results revealed the formation of an incomplete platinum film after a deposition time of 2 h (platinum and silicon signals were detected) and a dense platinum film that entirely covered the glass substrate after 22 h because pronounced platinum signals were measured while no silicon signal from the glass substrate was detectable anymore. The Pt 4f spectrum was characterized by an intense component at 71.8 ± 0.2 eV assigned to the platinum in the elemental state accompanied by less intense signals at 73.2 ± 0.2 and 74.6 ± 0.2 eV ascribed to residues of the precursor and to traces of platinum oxides or hydroxides. This is in line with a Cl $2p_{3/2}$ signal at 199.0 ± 0.2 eV and with the oxygen spectrum that is composed of two components at 532.0 ± 0.2 and at 533.7 ± 0.2 eV.

As a result of the dense packing of the platinum nanoparticles, the platinum films were electrically conducting. The sheet resistivity (ρ_s) of the films could be controlled by applying different deposition conditions, e.g., time, as illustrated in Figure 5a, which shows a reduction of ρ_s by more than 3 orders of magnitude with increasing deposition time in as-deposited films. This decrease might be caused by somewhat larger nanoparticles (less grain boundaries) or an increased percolation path. Being able to tune ρ_s over such a wide range is, of course, beneficial and usually not possible with other deposition methods. Additionally, the sheet resistivity could be further decreased by annealing the films (Figure 5a), probably because of partial sintering or Ostwald ripening (14) of the platinum particles. The sheet resistivity of the electroless-deposited platinum films resembles the one measured on a 50-nm-thick thermally evaporated platinum film, as shown in Figure 5a.

The low resistivity was preserved upon sonication of the films in toluene for 15 min. Also, upon repeated peeling with Scotch tape, ρ_s remained essentially constant, as shown in Figure 5b, although part of the platinum film was transferred to the Scotch tape after peeling for the first few times. This indicates that the topmost platinum layer is loosely bound, but the underlying film, responsible for the high conductivity, adhered well to the substrate.

The proposed chemical reaction, leading to a reduction of the precursor to metallic platinum and finally to a film, is given in eq 1. Dissolved *cis*-$[PtCl_2(sty)_2]$ is in equilibrium with *trans*-$[PtCl_2(sty)_2]$ and $[Pt_2Cl_4(sty)_2]$ (15), and ^{195}Pt NMR spectra revealed the presence of $[Pt_2Cl_4(sty)_2]$ with less than 10% *trans*-$[PtCl_2(sty)_2]$ in the seed solution. The formation of the trans isomer appears important for further reaction: experiments with $[Pt_2Cl_4(sty)_2]$ dissolved in toluene did not yield a platinum film, while the addition of styrene (e.g., 2 equiv), which in situ formed *trans*-$[PtCl_2(sty)_2]$, led to film formation after a variable induction period.

$$2\,cis\text{-}[PtCl_2(sty)_2] \rightleftharpoons \begin{cases} trans\text{-}[PtCl_2(sty)_2] \\ [Pt_2Cl_4(sty)_2] + 2(sty) \end{cases} \xrightarrow[\text{of toluene}]{\text{methyl group}} 2Pt + 4HCl\uparrow + 4(sty) \quad (1)$$

Most remarkably, an isotope effect revealed that toluene's methyl group is involved in the reaction because neither toluene-d^8 (completely deuterated) nor toluene-d^3 (deuterated methyl group) formed a film, while, on the other hand, toluene-d^5 (deuterated phenyl ring) resulted in film formation. Deuteration of the styrene molecules in *cis*-$[PtCl_2(sty)_2]$ also had no influence on film formation. This indicates that chloride is finally eliminated, likely as HCl, because a pH indicator paper fixed in the lid of the glass vessel showed that an acid evolved during the reaction. By mixing toluene with 1,2-dicholorobenzene, which by itself dissolves *cis*-$[PtCl_2(sty)_2]$ but does not lead to film formation, it was found that the time to form a film depends linearly on the toluene concentration. Therefore, it seems that toluene's methyl group is directly involved in the reduction of platinum(II) and does not act as a catalyst.

In conclusion, we have presented a simple and robust electroless deposition process for the manufacture of flexible platinum films and mirrors in which the precursor *cis*-$[PtCl_2(sty)_2]$ is converted in toluene at 80 °C or above to a nanoporous, electrically conducting platinum film on a very broad range of substrates. The ultrathin films are comprised of ligand-free nanoparticles with 1 nm diameter in the primary film and 3−5 nm diameter in the secondary film. The films adhere well to the substrates, they can be deposited with varying transparency, and they are highly conducting with a tunable sheet resistivity of over 5 orders of magnitude. The uncommon versatility of substrates of completely different chemical composition that can be coated is apparently due to the ability of the precursor to adsorb onto or react with surfaces of different chemical nature, either by coordination (styrene can readily be exchanged (16)) or by van der Waals attraction. An isotope effect indicated that the solvent's methyl group reduces the *cis*-$[PtCl_2(sty)_2]$ precursor above 80 °C, leading to a release of the ligands, which yields crystallization nuclei in the solution as well as at surfaces in contact with the solution.

EXPERIMENTAL SECTION

Syntheses. *cis*-$[PtCl_2(sty)_2]$ was synthesized according to ref 16. In a beaker (250 mL), platinum(II) chloride (Johnson Matthey; 7.48 g, 28.1 mmol) and freshly distilled (60 °C, 20 mbar) styrene (Sigma-Aldrich ReagentPlus; 180 mL, 1.57 mol, 55.7 equiv) were stirred at room temperature for 72 h or more. The reaction mixture was then filtered and washed with benzene (100 mL) and subsequently with pentane (150 mL). The remaining yellow solid was dried under vacuum (≈10 mbar, 24 h) to yield 10.22 g (77%) of the desired product.

cis-$[PtCl_2(sty\text{-}d^8)_2]$ was synthesized by replacing styrene in the above recipe with undistilled perdeuterated styrene.

$[Pt_2Cl_4(sty)_2]$. *cis*-Dichlorobis(styrene)platinum(II) (4.01 g, 8.5 mmol) was dissolved in chloroform (40 mL) in a round-bottomed flask (250 mL) (16). After heating under reflux at 70 °C for 90 min, the reaction mixture was cooled to room temperature and the precipitate was dissolved with dichloromethane (40 mL). The mixture was then filtered, and the solvent was concentrated under reduced pressure to about 10 mL. The addition of pentane (50 mL) and storage at 4 °C overnight led to precipitation. Filtration, washing with pentane (70 mL), and drying under a vacuum (≈10 mbar) led to 2.90 g (92%) of the desired product as a red solid.

Thin-Film Formation. In a typical experiment, 75 mg of *cis*-$[PtCl_2(sty)_2]$ were dispersed in 15 mL of toluene at room temperature without stirring in a cylindrical glass vessel (30 mL, VWR), which was used as received without further cleaning. The resulting yellow dispersion turned to an orange solution after a few minutes when heated to 80 °C. This color change is most likely due to the formation of di-μ-chlorodichlorobis(styrene)diplatinum(II) (^{195}Pt NMR, 200 K, δ −2303, −2334, and −2370) and only partly caused by the formation of *trans*-$[PtCl_2(sty)_2]$ (^{195}Pt NMR, 200 K, δ −2647). The film formation is insensitive to toluene's quality, and technical-grade as well as analytical-quality (>99.7%) or anhydrous toluene yielded equivalent results. The solvent-cleaned (acetone, 2-propanol, and/or toluene) substrates to be platinized (typical dimensions 9 × 25 mm) were fixed in a Teflon holder and immersed into the hot, orange solution. After some minutes brown, cloudy precipitates started to form, which accumulated at the bottom of the vessel. After heating for ≈20 h, a further color change occurred from clear orange to brown/orange within less than 1 h, which indicates the presence of nanoparticles (17). Additionally, the precipitates lost their cloudy structure and became denser and darker (dark brown). We refer to the solution in this state as a *seed solution*.

After heating for 22−24 h, a semitransparent, brown *primary film* formed on the walls of the glass vessel and on immersed substrates, and the precipitates became more dense, until small black particles sedimented on the bottom of the glass vessel. XRD identified this black powder as elemental platinum with a particle size of 2−3 nm (platinum black). The powder appeared to be rather pure because only small residues of C (0.87%), H (0.01%), N (0.05%), and Cl (0.8%) were found.

Upon further heating, the deposited films became shinier and opaque, denoting the formation of the *secondary film*. The so-deposited films appeared bright and silver shiny when inspected from inside the glass vessel (surface that grew last), while it appeared darker from the outside (surface that grew first). After annealing at, e.g., 200 °C for 10 min, both surfaces appeared very silvery and shiny. In experiments where the seed solution

was transferred to a new glass vessel, a platinum film formed within 24 h at 80 °C, which indicates that the glass surface was not modified by reactions in the first 20 h; thus, when the seed solution is prepared in advance, the time to platinize samples can be reduced significantly. We note that the presented platinization process allows easy recycling of the platinum powder and of platinum films deposited on surfaces other than the samples, thereby enabling a platinum usage close to 100%.

Films on the polymer electrolyte membrane (13) (pyridine content ≈ 60%) were deposited either on washed membranes (4 h, 80 °C, toluene) or on pretreated membranes (24 h at 85 °C, 72 h at 110 °C, phosphoric acid). Platinized membranes could be immersed in hot phosphoric acid without visually harming the platinum films, and they also remained conducting.

Cross-Sectional TEM. The platinum-coated Kapton foil was glued with a two-component epoxy glue between two silicon wafer pieces and embedded with the same glue in a copper tube. Thin slices of this tube (0.4 mm) were ground and polished by hand to a disk with a thickness of 0.1 mm using sandpaper of different grades. A recess was made on each side of the disk with a Gatan 656 dimple grinder to obtain a ≈20-μm-thick membrane, which was then etched in a Gatan 691 Precision Ion Polishing System with two focused argon-ion beams (etching angle 4°; acceleration voltage 4.3 kV) until a hole was obtained. At the edge of the hole, the sample was transparent for electrons. TEM micrographs were recorded using a Philips CM30ST transmission electron microscope with an acceleration voltage of 300 keV (point-to-point resolution 0.19 nm).

A carbon-coated TEM grid was platinized using typical experimental conditions for 20 h. The platinum film was already too thick to be imaged with TEM, but part of the carbon membrane ruptured and coiled up, thereby providing a virgin surface for a new platinum film to grow for an unknown time and enabling imaging of a cross section, hence the three-dimensional form of the nanoparticle clusters.

Other Measurements and Materials. The XPS spectra were measured on a PHI Quantera Scanning X-ray Microprobe using a monochromatic 100-μm Al Kα source. The residual pressure in the spectrometer was always below 5×10^{-7} Pa. The system was calibrated according to ISO 15472:2001 with an accuracy of ±0.1 eV.

The XRD spectra were measured on a PANalytical X'Pert Pro diffractometer equipped with a Cu Kα source and an X'Celerator detector.

The sheet resistivity was measured in a linear four-point configuration with an Agilent 4155C semiconductor parameter analyzer and calculated according to ref 18 using $\rho_s = \Delta V \pi / I / \ln 2$, where I denotes the current passed through the two outer electrodes and ΔV the voltage drop measured between the two inner electrodes.

The porous PTFE was obtained from ElringKlinger (Zenith A, 1 mm thick). The polystyrene was cross-linked by mixing 5 mL of distilled styrene with 300 mg of distilled divinylbenzene and 170 mg of dibenzoyl peroxide. This solution was dried in an aluminum dish on a hot plate at 80 °C under nitrogen flow.

For qualitative adhesion tests, Scotch tape 810 was firmly pressed onto films and slowly peeled off afterward.

Acknowledgment. The authors express their sincere gratitude to Paul Smith and the Geordies' crew for their support. We further thank E. Barthazy, E. Müller, and P. Wägli of the Electron Microscopy group of ETH Zurich (EMEZ) for TEM and SEM investigations, M. Niederberger and D. Koziej for access to their X-ray diffractometer, J. Kallitsis for supplying the polymer electrolyte membrane, and H. Rüegger for NMR measurements.

REFERENCES AND NOTES

(1) Seydel, W. *Kunstbuch oder von manigerlai Handwerchskünsten, handwriting*; Tegernsee, Bayerische Staatsbibliothek: 1550; Cgm 4117.
(2) Beckmann, J. *Beyträge zur Geschichte der Erfindungen*; Paul Gotthelf Kummer: Leipzig, Germany, 1782; Vol. 1.
(3) Liebig, J. *Ann. Pharm.* **1835**, *140*, 133–167.
(4) Okinaka, Y., Wolowodiuk, C. In *Electroless Plating - Fundamentals and Applications*; Mallory, G. O., Hajdu, J. B., Eds.; William Andrew Publishing/Noyes: 1990; pp 421−440.
(5) Gorostiza, P.; Servat, J.; Morante, J. R.; Sanz, F. *Thin Solid Films* **1996**, *275*, 12–17.
(6) Rao, C. R.; Trivedi, D. *Coord. Chem. Rev.* **2005**, *249*, 613–631.
(7) Kim, Y.-T.; Ohshima, K.; Higashimine, K.; Uruga, T.; Takata, M.; Suematsu, H.; Mitani, T. *Angew. Chem., Int. Ed.* **2006**, *45*, 407–411.
(8) Cui, G.; Zhi, L.; Thomas, A.; Kolb, U.; Lieberwirth, I.; Müllen, K. *Angew. Chem., Int. Ed.* **2007**, *46*, 3464–3467.
(9) Yang, D.-Q.; Sun, S.; Dodelet, J.-P.; Sacher, E. *J. Phys. Chem. C* **2008**, *112*, 11717–11721.
(10) Kamperman, M.; Burns, A.; Weissgraeber, R.; van Vegten, N.; Warren, S. C.; Gruner, S. M.; Baiker, A.; Wiesner, U. *Nano Lett.* **2009**, *9*, 2756–2762.
(11) Xie, J.; Zhang, Q.; Zhou, W.; Lee, J. Y.; Wang, D. I. C. *Langmuir* **2009**, *25*, 6454–6459.
(12) Peng, K.-Q.; Wang, X.; Wu, X.-L.; Lee, S.-T. *Nano Lett.* **2009**, *9*, 3704–3709.
(13) Pefkianakis, E. K.; Deimede, V.; Daletou, M. K.; Gourdoupi, N.; Kallitsis, J. K. *Macromol. Rapid Commun.* **2005**, *26*, 1724–1728.
(14) Ostwald, W. *Z. Phys. Chem.* **1900**, *34*, 495–503.
(15) Caseri, W.; Pregosin, P. S. *Organometallics* **1988**, *7*, 1373–1380.
(16) Albinati, A.; Caseri, W. R.; Pregosin, P. S. *Organometallics* **1987**, *6*, 788–793.
(17) Gianini, M.; Caseri, W. R.; Suter, U. W. *J. Phys. Chem. B* **2001**, *105*, 7399–7404.
(18) Blythe, T.; Bloor, D. *Electrical Properties of Polymers*; Cambridge University Press: Cambridge, U.K., 2005.

AM900918Y